International Journal of Rock Mechanics & Mining Sciences 170 (2023) 105480

Contents lists available at ScienceDirect

International Journal of Rock Mechanics and Mining Sciences

journal homepage: www.elsevier.com/locate/ijrmms

A bulking model to simulate stope convergence in deep tabular excavations

Y. Jooste, J.A.L. Napier, D.F. Malan *

Department of Mining Engineering, University of Pretoria, South Africa

ARTICLE INFO

Keywords:
Stope convergence
Tabular stope
Displacement discontinuity modelling

ABSTRACT

This paper investigates the use of a novel time-dependent bulking model in a displacement discontinuity code to simulate the convergence between the roof and the floor of deep tabular stopes. This study is important as the current layout design criteria that are based on elastic theory have become outdated. This approach ignores rock failure and fails to predict the actual magnitude and the time-dependent nature of the stope convergence. This has implications for support design and for estimating the stress acting on remnants in mature mines. A rock mass modulus reduction strategy, often used to circumvent this problem, reflects the expected lower effective rock modulus for near-stope fractured material, but must be applied for the entire rock mass region in the displacement discontinuity solution procedure for tabular layout problems. As an alternative, it is proposed in this paper that the rock bulking can be expressed as a function of the elastic closure by using a constitutive rule for the reef-normal compressive reaction stress that is expressed as a function of the compaction strain. The proposed model was tested using convergence data collected from a shaft pillar extraction in a deep gold mine. The bulking model, in conjunction with a limit equilibrium model to simulate the face crushing, seems capable of replicating the underground behaviour. As the stresses on remnants and pillars can be more accurately simulated, this approach holds promise of improving current design criteria. Calibration of the model nevertheless remains a challenge and a programme of routine convergence measurements will have to be implemented on the mines.

1. Introduction

The deep gold mines in the Witwatersrand Basin in South Africa have yielded over 52 000 tonnes of gold and this represents more than one third of all gold ever produced on the planet. It is estimated that an inferred resource of about 30 000 tonnes remains in the basin.[1] As discussed by Malan and Napier[2], the shallow dipping nature of the deep tabular orebodies presents many rock engineering challenges. Owing to the great depths of the mining operations, the stopes are seismically active and rockbursts and falls of ground were the cause of many fatalities during the early years of mining. Although the safety record of the mines has improved significantly in recent years[3], the development of updated design criteria for these deep tabular layouts is urgently required. Remnants and pillars are mined in many of the older operations and there is a need to improve the criteria used to select which of these remaining blocks of ground can be safely extracted.

The current layout design criteria are based on elastic theory and the failure of the rock mass is not considered. The historic development of these elastic criteria is described in detail in a number of references.[3,4]. Denkhaus et al.[5] note that a research team from the CSIR in South Africa was commissioned in 1952 to investigate the rock stress problem at depth. They proposed that the overall rock mass deformations and stress redistribution around deep level tabular mine excavations could be based on the assumption that the rock mass behaves as an elastic continuum. This theory was based on laboratory compression tests performed on rock specimens from the Witwatersrand Basin which indicated that rock behaves essentially elastically up to the point of failure. There were also earlier papers from other countries that applied elastic theory to mining problems.[6]

The adoption of the elastic concept was reinforced by a set of measurements conducted by Ryder and Officer.[7] They measured the rock mass deformation in the hangingwall and footwall near two adjacent longwall stopes at East Rand Proprietary Mines (ERPM) from 1961 to 1963. The graphs published in their paper are historically significant as it was the first attempt to compare theoretical elastic displacements in the rock mass with actual movements observed in the vicinity of a deep-level longwall. Based on these results, the authors concluded that the observed displacements in the rock mass remote from mining excavations are essentially in agreement with elastic theory. It was also stated that the elastic constants determined from small specimens

* Corresponding author.
E-mail address: francois.malan@up.ac.za (D.F. Malan).

https://doi.org/10.1016/j.ijrmms.2023.105480
Received 21 September 2022; Received in revised form 16 April 2023; Accepted 20 June 2023
Available online 24 June 2023

appear to be a good estimate of the properties of the rock mass underground. Ortlepp and Cook[8] used a similar simplified two-dimensional elastic solution to compare measurements close to a longwall at Harmony Gold Mine using elastic theory. Ortlepp and Nicoll[9] extended the work by using an electrical analogue to simulate the rock movements at Harmony Gold Mine and ERPM. Cook et al.[10] summarized the progress at that stage by noting that the intact rock mass behaves elastically, while seismic observations have indicated that there is close agreement between active mining operations and releases of energy.

A further development that made the simulation of stress distributions around tabular excavations possible was a suggestion by Hackett[11] that a parallel-sided panel geometry in a coal mine can be considered to be analogous to a crack in an elastic rock mass. This work was followed by the work of Berry[12,13] and Berry and Sales[14,15] which laid the theoretical foundation for the numerical boundary integral equation technique which is now known as the Displacement Discontinuity Method (DDM). Berry[12] acknowledges the contribution of Prof. R. Hill who was apparently responsible for the fundamental idea of representing a tabular excavation as a dislocation in an elastic medium. A similar concept was introduced in South Africa by the papers written by Salamon[16–19] and this was termed the "*Face Element Principle*". The displacement discontinuity technique was implemented in numerical computer codes in the late 1960s when mainframe computers became available.[20,21] A description of the popular South African tabular mine design tool, known as MINSIM, which was developed at the Chamber of Mines of South Africa Research Organisation (COMRO) was published by Deist et al.[22]

The adoption of elastic theory and the simulation of the layouts using the displacement discontinuity method enabled the development of a number of design criteria for the deep gold mines. The two most widely used criteria are average pillar stress (APS)[23] and energy release rate (ERR).[24] These criteria have been useful for many decades and have assisted mine planners to reduce excessive stress concentrations and to identify the most favourable mining sequences. These criteria have contributed to a significant improvement in safety since 1994.[3] A drawback of these criteria is the underlying assumption of an isotropic, homogenous elastic rock mass which ignores the fracture envelope near the edges of deep stopes.[25] Measurements of the convergence between the roof and floor in tabular excavations have highlighted the effect of the facture zone and this is described in the next section.

2. Stope convergence measurements and inelastic rock behaviour

The early 1975 ISRM definitions for convergence and closure will be adopted in this paper[26]. This differs from the conventions gradually adopted in the South African mining industry, but simplifies the description of the proposed bulking model. For the purposes of this paper, c*onvergence* in a tabular excavation is the relative movement of the hangingwall and footwall normal to the plane of the reef. This consists of an elastic component, called *elastic convergence*, and an inelastic component caused by the rock fracture process and associated movements. *Closure* occurs when the magnitude of convergence equals the stoping width and contact occurs between the hangingwall and footwall of the excavation. Closure is frequently encountered in the deep tabular stopes in areas where the excavation spans are large. Fig. 1 illustrates an example of closure and, as a result, the timber support pack is compressed to a negligible height. This pack would have had the same installed height as the newly installed packs in the figure. Note the cable, used for the cleaning scraper in the old stope, seemingly protruding from the rock face. The fractured nature of the hangingwall and footwall is evident and this material must be re-compacted before substantial load is carried by these zones of contact.

Some of the earliest references to convergence measurements in South African gold mines can be found in papers by Altson[27] and Mickel[28]. Prominent time-dependent convergence between successive face blasts was therefore recorded as early as the 1930s. A recently recorded example of this convergence behaviour is given in Section 4 below. Leeman[29] conducted extensive measurements of convergence at ERPM. He used instruments that recorded the convergence in a continuous fashion between the footwall and hangingwall of the stope. This work confirmed that movements in the fractured rock mass surrounding the stopes results in time-dependent convergence behaviour. Evidence that the fractured rock mass, consisting of a hard-brittle material, behaves in a creep-like fashion was a major discovery by these workers. Roux and Denkhaus[30] also hypothesised that the rock mass behaves in a time-dependent fashion as rockbursts frequently occurred several hours after blasting when no changes in geometry occurred.

Hodgson[31] collected convergence data at ERPM and referred to the successful use of elastic theory to describe the far field rock mass behaviour and the value of the design criteria proposed on this basis. He nevertheless noted: "*The observations have shown that the most important property of the failed zone is time-dependent behaviour and that this behaviour is of direct concern to practical problems of designing* support*, face advance per blast and frequency of blasting so as to minimize the rockburst problem or, at least avoid aggravating it.*" This was a profound statement, but unfortunately systematic continuous convergence measurements and the time dependent nature of the rock mass were only resumed again in the 1990s.[32,33] The reason for this was probably that elastic theory was already deeply entrenched by the late 1960s and research efforts were directed to develop numerical codes that can simulate irregular tabular layouts in an elastic medium.

The adoption of elastic theory was found to be problematic when researchers attempted to reconcile actual underground convergence measurements with numerical simulations. Walsh et al.[34] conducted convergence measurements at West Driefontein Gold Mine. His data illustrated that the observed convergence magnitude is significantly larger than that predicted by elastic theory. These authors ascribe the

Fig. 1. A deep tabular gold mine stope illustrating typical timber support packs (left). These packs are compressed to a small width if closure occurs (right). (For interpretation of the references to colour in this figure legend, the reader is referred to the Web version of this article.)

discrepancy to inelastic movements on discontinuities in the hanging-wall and footwall. Gurtunca and Adams[35] recorded convergence in stopes supported by backfill. The recorded convergence magnitude was found to be significantly higher than that predicted by numerical codes when using a Young's modulus of 70 GPa for the assumed elastic rock mass. They recommended the use of a reduced *in situ* Young's modulus with values between 40 GPa and 70 GPa to simulate the observed convergence. Gurtunca and Adams[35] note in their paper that: "*The use of an in situ modulus provides an effective interim solution until a new computer model that allows for joints, different layers, and inelastic closures becomes generally available*." This proposal was widely critised[36], but practising rock engineers in the South African gold mining industry routinely use a lower Young's modulus compared to the values obtained from laboratory testing.

This dilemma has persisted as a suitable model to simulate the inelastic failure processes and the time-dependent convergence was never developed. Elastic theory and the displacement discontinuity method made the simulation of stress and displacement for large scale irregular-shaped tabular geometries possible. This was a major leap forward and the effect of the fracture zone has been ignored generally for mine-scale simulations. In this paper an alternative constitutive model, for use with the displacement discontinuity method, is proposed. This retains the powerful attributes of the original approach, but it allows for the simulation of more realistic convergence values and the effect of closure on pillar stress. The time-dependent convergence behaviour observed in the stopes can also be simulated.

3. A proposed bulking model to simulate stope convergence behaviour

The modulus reduction strategy reflects an expected lower effective rock modulus for near-stope fractured material but must be applied over the whole rock mass region. A mechanism-driven model should attempt to consider both the local fracture zone and parting plane deformations to encapsulate the near-face convergence rate and the large-scale rock mass behaviour. Salamon[37] suggested a compaction model to predict the height of caved rock in the "goaf" areas of longwall coal mines. This model considers the initial equilibrium of a vertical pile of caved material that is compacted under gravitational forces. The model assumes a hyperbolic relationship between the vertical stress and the void ratio at each level of the caved material above the excavation footwall. The model does not consider the open span between the mining face and the point at which closure occurs and is not related to the evolution of the reaction stress in the caved region as mining progresses.

An alternative model to represent the back-area caving evolution is outlined in this paper. Assume that the tabular mining excavation falls in a local x-y plane with the mining height in the z-coordinate direction (see Fig. 2).

Suppose that the rock bulking can be expressed as a function of the distance to the mining face or as a function of the elastic convergence D_z. For the second option, assume that the observed convergence, D_z^{obs}, is given by

$$D_z^{obs} = B_f D_z \tag{1}$$

where B_f is a specified bulking factor. This is illustrated schematically in Fig. 3 where the elastic convergence D_z and observed convergence D_z^{obs} are plotted as functions of the distance x from the mining face. The diagram in Fig. 3 requires some clarification. The elastic convergence behaviour of tabular stopes, similar to the geometry illustrated in Fig. 2, has been studied extensively. A two-dimensional elastic convergence solution for a parallel-sided stope in an isotropic elastic rock mass can be found in several publications[2,23,38]. The derivation of this solution assumes that the stope can be approximated as a slit or crack with no mining height. The seam is not allowed to deform. The solution predicts that the convergence at the stope face is nil and it increases as the distance to face increases. The convergence profile D_z , shown in Fig. 3, can for example be obtained by plotting the convergence equation given in Malan and Napier[2].

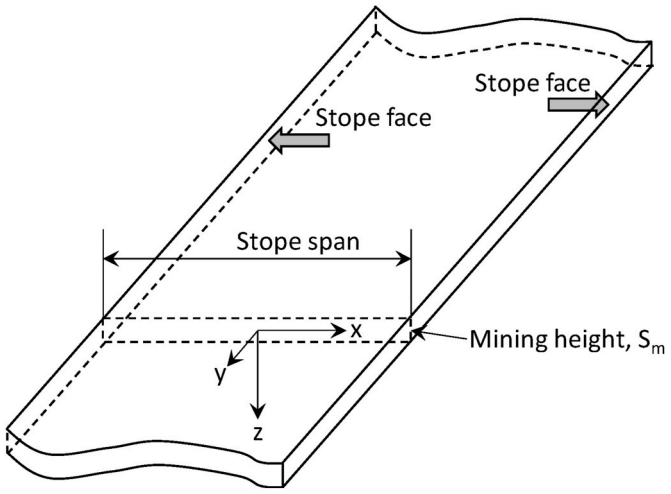

Fig. 2. A parallel-sided tabular stope illustrating the coordinate system and the mining height.

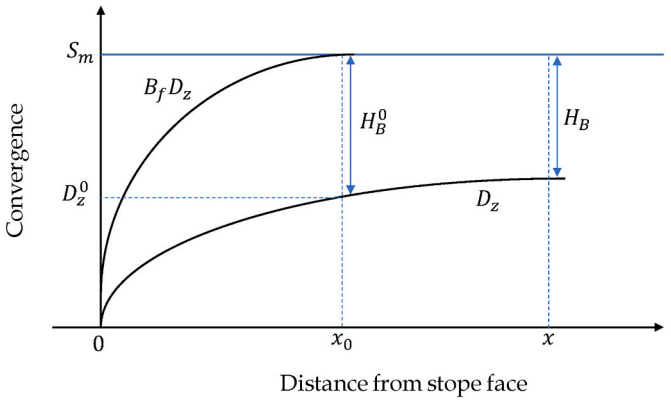

Fig. 3. Conceptual closure profiles in bulked rock expressed as a function of the distance from the stope face.

Let D_z^0 and H_B^0 represent respectively the elastic convergence and the unconsolidated bulked material height at the point of first contact $x = x_0$ as shown in Fig. 3. If the mining height is S_m then

$$S_m = H_B^0 + D_z^0 = B_f D_z^0 \tag{2}$$

and

$$D_z^0 = \frac{S_m}{B_f} \tag{3}$$

From Eqs. (2) and (3), it follows that

$$H_B^0 = \frac{(B_f - 1)S_m}{B_f} \tag{4}$$

It should be noted that $H_B^0 = 0$ when $B_f = 1$ and that $H_B^0 \rightarrow S_m$ if B_f is very large consequently imposing an upper limit on the bulking zone height.

When $x > x_0$ it is assumed that the bulked material becomes reconsolidated. The vertical compression of the bulked material in this region is $H_B^0 - H_B$ where $H_B = S_m - D_z$ and $D_z \geq D_z^0$ The vertical strain, ε, in the bulked material relative to the initial height of the unconsolidated material can be expressed as

$$\varepsilon = \frac{H_B^0 - S_m + D_z}{H_B^0} = \frac{D_z - D_z^0}{(B_f - 1)D_z^0} \tag{5}$$

Some constitutive rule has to be postulated to determine the reef-normal compressive reaction stress R as a function of the strain. Employing Eq. (3), it can be seen from Eq. (5) that $\varepsilon = 0$ when $D_z = D_z^0$ and that $\varepsilon = 1$ when $D_z = S_m$. Using a hyperbolic consolidation model which recognises these strain limits it is postulated that

$$R(\varepsilon) = \frac{E_0 \varepsilon}{1 - \varepsilon} \tag{6}$$

and

$$\frac{dR}{d\varepsilon} = \frac{E_0}{(1 - \varepsilon)^2} \tag{7}$$

where E_0 is the initial reconsolidation modulus in the bulked material when $\varepsilon = 0$. It should be noted that Eq. (6) is based on the postulation that the re-compaction of the bulked material obeys the familiar 'hyperbolic backfill' relationship[23]. This constitutive law has been adopted in the South African gold mines to describe the behaviour of backfill when subjected to stope convergence and has been confirmed using underground and laboratory measurements. This model can describe the behaviour of a variety of backfill materials, even for milled waste rock, and it is therefore considered to be a good assumption for the compaction of fractured rock.

The convergence distribution at all points of the tabular layout is determined by tessellating the excavation region with triangular or quadrilateral displacement discontinuity boundary elements as described, for example, by Napier and Malan[39]. Eq. (6) can be used to determine the value for the elastic closure component D_z at each element collocation point within the iterative solution structure for the displacement discontinuity element ensemble. The details of these iterative solution methods are beyond the scope of this paper and readers are advised to consult the numerous publications in this regard[21,22,39]. Specifically, the solution value is determined by repetitively solving the equilibrium relationship for the reef-normal stress component

$$-R(\varepsilon) = K_z D_z + E_z \tag{8}$$

where K_z is the collocation point self-effect stiffness and E_z represents the iteratively updated sum of all external stress and primitive stress values induced by the surrounding collocation point values. Note that compressive stress values are assumed to be negative on the right-hand side of Eq. (8). Substituting Eq. (6) into Eq. (8) gives the following:

$$-\frac{E_0 \varepsilon}{1 - \varepsilon} = K_z D_z + E_z \tag{9}$$

By inserting Eq. (5), it follows that:

$$-\frac{E_0 (D_z - D_z^0)}{B_f D_z^0 - D_z} = K_z D_z + E_z \tag{10}$$

Furthermore, Eq. (3) can be inserted:

$$-\frac{E_0 (D_z - D_z^0)}{S_m - D_z} = K_z D_z + E_z \tag{11}$$

This gives

$$-E_0 (D_z - D_z^0) = (S_m - D_z)(K_z D_z + E_z) \tag{12}$$

which results in the following quadratic equation for D_z:

$$D_z^2 - b_Q D_z + c_Q = 0 \tag{13}$$

where

$$b_Q = \frac{E_0 + S_m K_z - E_z}{K_z} \tag{14}$$

and

$$c_Q = \frac{E_0 D_z^0 - S_m E_z}{K_z} \tag{15}$$

The appropriate solution branch ensuring that $D_z^0 < D_z < S_m$ is given by

$$D_z = \frac{b_Q - \sqrt{b_Q^2 - 4c_Q}}{2} \tag{16}$$

As significant time-dependent convergence is recorded in the underground stopes, an initial approach to allow time-dependent bulking in the mined region is to postulate that B_f follows a time dependent evolution between a specified initial value B_f^0 and maximum value B_f^m. This relationship is assumed to be of the form

$$B_f = B_f^m - \left(B_f^m - B_f^0\right)\left(\frac{1}{2}\right)^{T/\lambda_B} \tag{17}$$

where T is the elapsed time from the time that the excavation is formed and λ_B is a bulking expansion half-life parameter. Eq. (13) takes the limiting values $B_f = B_f^0$ when $T = 0$ and $B_f = B_f^m$ as $T \to \infty$. It should be noted that $\left(\frac{1}{2}\right)^{T/\lambda_B} = e^{-\alpha T}$ where $\lambda_B = \frac{ln(2)}{\alpha}$. This choice of exponential decay model for the rock is supported by the work presented in Malan and Napier[41]. They recorded and simulated time-dependent closure profiles in gold mine stopes. Exponential decay is also very common in nature of which the well-known example is radioactivity. It is therefore considered to be a reasonable assumption to represent the time-dependent bulking behaviour.

The model above was implemented in the TEXAN displacement discontinuity code[39]. Descriptions of the code are also given in Napier and Malan[40]. It is assumed provisionally that the value of B_f determined by Eq. (17) is not altered when a state of closure is reached at any point in the excavation. This implies that the value of H_B^0 given by Eq. (4) will vary with time at all points of the excavation and that this variation is not altered at back area positions where closure occurs. This assumption may possibly need to be reviewed depending on available calibration data or the formulation of a more elaborate mechanism-driven theory for the time-dependent bulking behaviour.

4. Data collected during the Bambanani shaft pillar extraction

The bulking model was tested using convergence data collected from instrumentation installed in a mining panel at Bambanani Gold Mine. The mine is a mature, deep-level mine located in the Welkom district of the Free State Province of South Africa. During the final stages of the life of mine, mining was limited to the extraction of the high-grade shaft pillar (the shaft was originally known as President Steyn No 4 Shaft). The shaft was sunk in 1968, with underground development commencing in 1972, and stoping following it in 1974. The recent shaft pillar mining was conducted at a depth of approximately 2219 m. The Basal Reef was extracted using conventional mini-longwall mining. The mini-longwall extraction method consists of follow-behind footwall development to extract the blasted ore through a system of ore passes, haulages and a decline system to the shaft. Given the high risk of seismicity, efforts were focused on rockburst resistant support systems[2], managing seismicity and the rehabilitation of areas with poor ground conditions. These challenges increased as the shaft pillar decreased in size. The shaft pillar mining was stopped during June 2022 and the mine was closed. The final mining outline of the pillar is shown in Fig. 4.

Monitoring of the seismic activity was an important part of the risk mitigating strategy and an extensive seismic network was installed. The

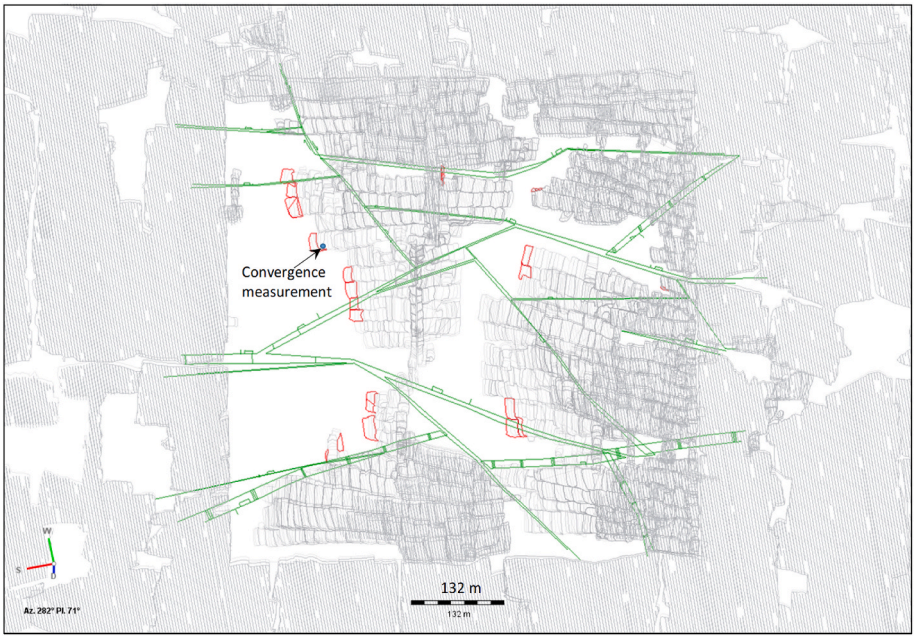

Fig. 4. Mining outlines and major geological structures in the Bambanani shaft pillar.

seismic system could record seismic events with magnitudes as low as $M_L = -2.0$ and the location error for a $M_L = 0.0$ event was approximately 15 m. Fig. 5 illustrates all events with $M_L > 0.0$ recorded during the extraction from 2010 to 2022. The colour indicates the time period of the event and the size of the sphere is proportional to the local magnitude, M_L. Most of the seismicity occurred close to the active mining faces. The mining sequence can therefore be identified with the mining starting on the right in 2010 and progressing to the left of the pillar. A few large events occurred in the back areas and these were associated with highly stressed pillars in these areas and the geological structures traversing these pillars. The increase in stress on these pillars with time were simulated and this is discussed below.

The conditions in the shaft pillar towards the end of the extraction period are shown in Fig. 6. Note the backfill support that is used to decrease the convergence and the associated magnitude of "released energy" as well as the use of steel wire rope netting to provide area coverage. During the final phases of mining, the stresses in the panel faces were high and this led to extensive crushing of the face as shown in the photograph. The nets used on the face were rolled back before blasting to prevent damage to these nets.

Panel convergence was recorded using telescopic instruments installed in the panels that could record the convergence in a continuous fashion. The convergence profiles recorded by these instruments have been described in detail in Malan[32] and Malan et al.[33]

Fig. 7 illustrates a typical convergence profile recorded by the instrument installed at the position shown in Fig. 4. At this position,

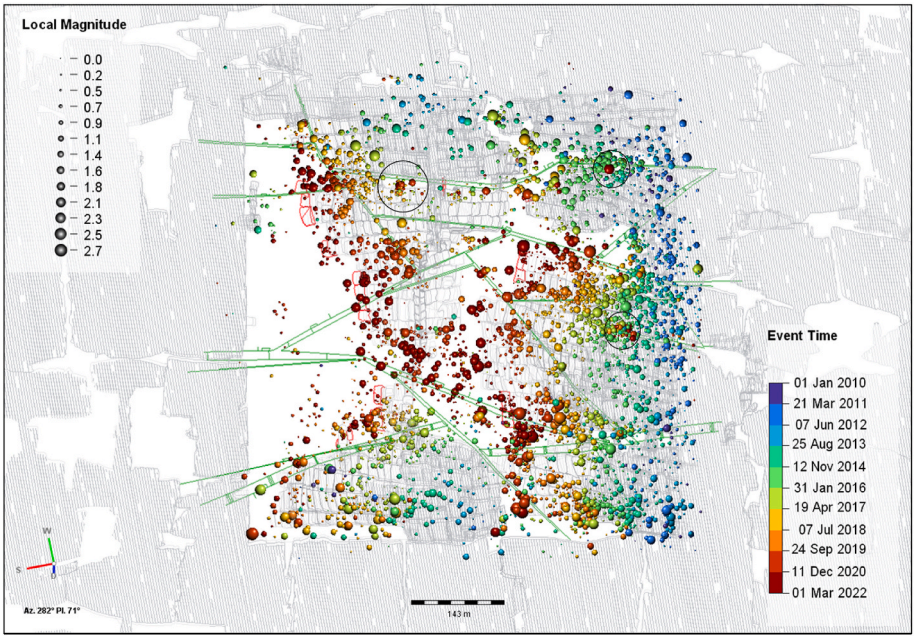

Fig. 5. A plot of the location of all seismic events with a $M_L > 0.0$ recorded from January 2010 to March 2022. The events associated with the pillars in the back areas are indicated by the black circles.

Fig. 6. Support used in the mining stopes in the Bambanani shaft pillar. The face of the panel is shown the right (covered by the net). Note the extensive crushing of the face.

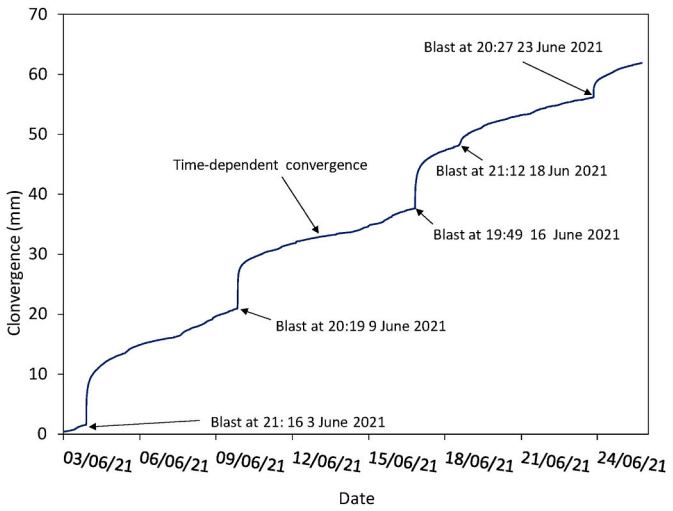

Fig. 7. Typical convergence profile recorded at the position indicated in Fig. 4.

approximately 62 mm of convergence was recorded over a period of 21 days. Similar to previous convergence profiles collected in these mines, the convergence is characterised by an instantaneous jump at blasting time followed by time-dependent convergence or "creep" that persists for many days in the absence of blasting.

For Eq. (17), a calibrated value for the bulking expansion half-life parameter, λ_B, is required. As discussed by Malan and Napier[41], the rate of time-dependent convergence between blasts appears to be constant in the short term, but decreases gradually when there is no blasting or seismic activity. It has been found that the time-dependent convergence or "steady-state convergence" can be approximated by a simple exponential decay function of the form[41]:

$$\Delta S_{ss} = a\left(1 - e^{-bt}\right) \tag{18}$$

where a and b are parameters and t is time. For the data from the Bambanani Shaft pillar (Fig. 7 for the steady-state closure after 10 June), the method of least squares was used to find the calibrated values for these parameters. This curve fitting can be easily done by using the "Solver" add-in utility in Excel. This gave values of $a = 3.91$ mm and $b = 0.0087$ h^{-1} with a correlation coefficient exceeding 0.9. To determine the half-life parameter the following equation can be used[41]:

$$\lambda_B = \frac{ln(2)}{b} \tag{19}$$

When inserting $b = 0.0087$ h^{-1}, it was found that $\lambda_B = 79.7$ h. This agrees with previous values obtained for different gold and platinum mines which ranged from 57.8 h to 192.5 h.[41].

5. Simulation of the Bambanani Shaft pillar

The proposed bulking model was tested by simulating the mining of the Bambanani Shaft pillar. The position of this shaft pillar, indicated by the red block, is shown relative to the stoped-out areas at the shaft in Fig. 8. This illustrates the extensive mined area surrounding the shaft pillar. For the TEXAN modelling, the mining outlines of the shaft pillar were approximated by straight line segments to simplify the digitising and element tessellation process. This is shown in Fig. 9. For the initial model, large annual mining steps - with the year 2017 as the baseline - were used to investigate the evolution of the loading stresses on the smaller pillars inside the shaft pillar. In some areas, small pillars were left between the panels. It is expected that these small pillars were crushed and therefore only the larger pillars were included in the model. In a particular year, mining was carried out in different areas in the shaft pillar and for each of these blocks a letter was added for example 2020a, 2020b, …2020j.

The sizes of the pillars are given in Table 1. The elastic and other modelling parameters are given in Table 2. Results from numerous overcoring stress measurements in South African gold mines indicated that the virgin vertical stress component typically increases according to the deadweight of the overburden. The virgin stress k-ratio (ratio of horizontal to vertical stress) tends to decrease with depth and typically has a value of 0.5 for the deep gold mines[25]. Note that the reef was simulated with no dip (the actual dip is ≈ 26°) and the pillar areas given in Table 1 are therefore slightly smaller than the actual sizes that were digitised using a plan view of the shaft pillar (the effect of ignoring dip is discussed below). The objective of the modelling was to test the new bulking model and therefore only an approximate layout was required. The depth of the shaft pillar at the top is approximately 1917 m and 2214 m at the bottom. A constant depth of 2500 m was, however, used for the modelling as extensive mining surrounds the shaft pillar (Fig. 8) and this results in an elevated stress magnitude. This "artificial" depth was determined by simulating a total area of 2 km x 2 km surrounding the shaft at the correct depth. When only simulating the shaft pillar of size 670 m x 615 m, a depth of 2500 m gave approximately similar stress values acting on this shaft pillar. The tabular reefs of the gold mines in South Africa persist for many kilometres in the lateral directions and selecting the appropriate domain size needs to be carefully weighed against the numerical modelling constraints caused by the maximum number of elements and realistic solution times. The domain size

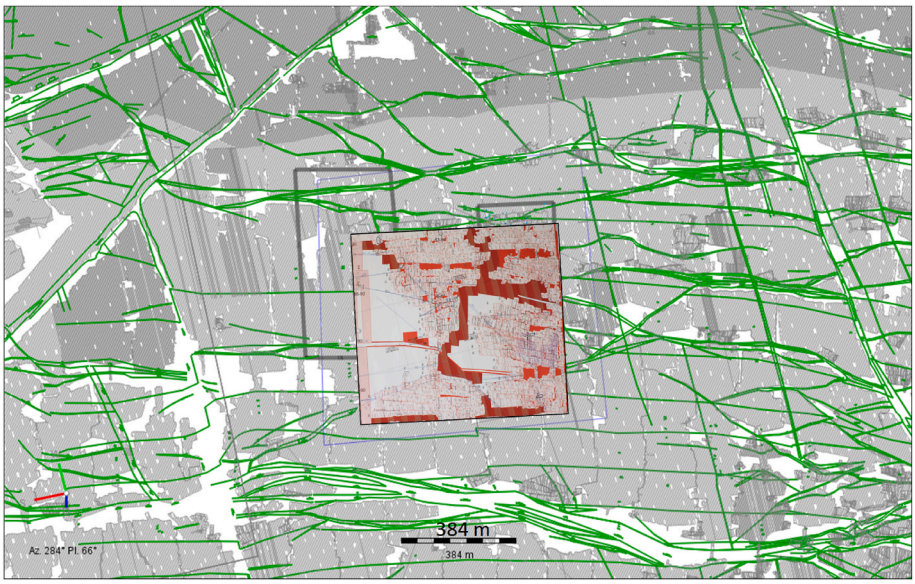

Fig. 8. Location of the Bambanani shaft pillar (red) relative to the other mined stopes (grey). Note the high extraction ratio in the surrounding mining areas. (For interpretation of the references to colour in this figure legend, the reader is referred to the Web version of this article.)

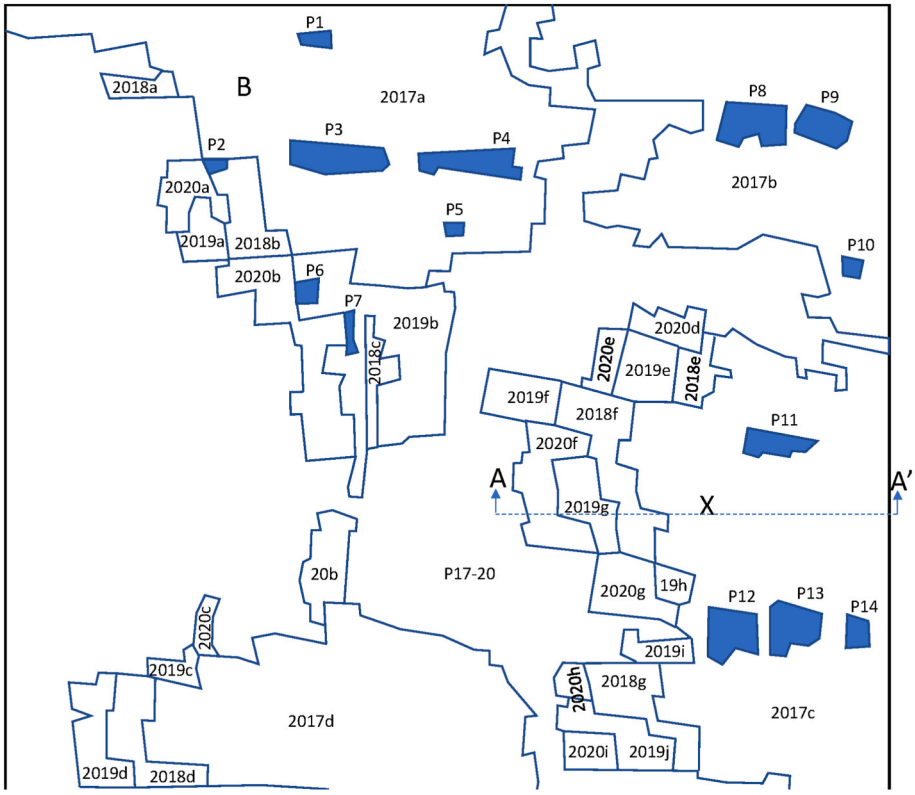

Fig. 9. Simplified mining outlines of the stopes and pillars in the Bambanani Shaft pillar. This is a plan view and illustrate the face positions during 2020. The size of the shaft pillar is 670 m along the horizontal axis and 615 m along the vertical axis.

selected for this paper was arbitrary as the objective was to illustrate the behaviour of the new constitutive model. Future work will have to carefully assess the size of the model required for improved calibration of the models.

The increase in stress that arises as mining progresses are given in Fig. 10 for the various pillars. These stress values represent the traditional APS criterion and were calculated as the average of the vertical stress values at each element collocation point falling within each pillar. The simulated stress magnitudes on some of the small pillars are very large and this will result seismic activity. It should be noted that the unrealistic high APS values, such as 654 MPa for pillar P7, are based on elastic modelling where the pillars are not allowed to fail. The small size of this pillar and the extensive mining result in these large simulated values. A traditional design rule in the deep gold mines is that APS $< 2.5 \times$ UCS, otherwise pillar foundation failure may occur[25]. For rock with a UCS $= 160$ MPa, this implies that the APS levels must remain below 400

Table 1
Pillar sizes.

Pillar	Size (m^2)	Pillar	Size (m^2)
P1	291	P10	230
P2	152	P11	804
P3	1458	P12	1276
P4	1329	P13	1274
P5	147	P14	416
P6	288	P17	98189
P7	228	P18	89385
P8	1472	P19	79087
P9	985	P20	68916

Table 2
Modelling parameters.

Parameter	Value
Young's modulus	70 GPa
Poisson's ratio	0.2
Overburden density	2700 kg/m^3
k-ratio (horizontal to vertical stress ratio)	0.5
Depth	2500 m
Average triangular element size	≈11.3 m^2
Dip of the reef	0°
Stoping width	1.5 m

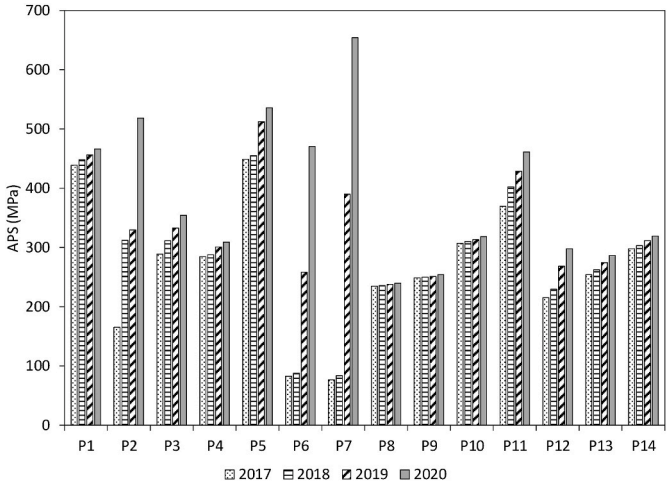

Fig. 10. Increase in pillars stress for the mining steps from 2017 to 2020.

MPa and pillar P7 exceeds this criterion. Pillar failure can be seen in Fig. 5 where large seismic events were triggered on some of the pillars in the back areas during 2020. This activity occurs in positions remote from the active mining faces and is a result of the increase in stress shown in Fig. 10.

To investigate the bulking model, the same geometry shown in Fig. 9 was simulated. The closure along Section AA' was calculated using different values of the Young's modulus (70 GPa and 35 GPa) with no bulking and bulking models with a Young's modulus of 70 GPa and B_f bulking factor values of 4, 6, 8 and 10. The time-dependent behaviour was not simulated for these initial runs and therefore $B_f^0 = B_f^m$. As a point of clarification, the complex model described further below also included a time-dependent limit equilibrium model to simulate the stope face fracturing. There are therefore two constitutive models, both with a time-dependent component, that can be used in combination in the TEXAN code, but these initial runs only tested the bulking model without any face fracturing or time-dependency. The convergence results are illustrated in Fig. 11. As expected, the elastic convergence increases for a lower value of Young's modulus. For the bulking model, the convergence increases for higher values of B_f until closure occurs as

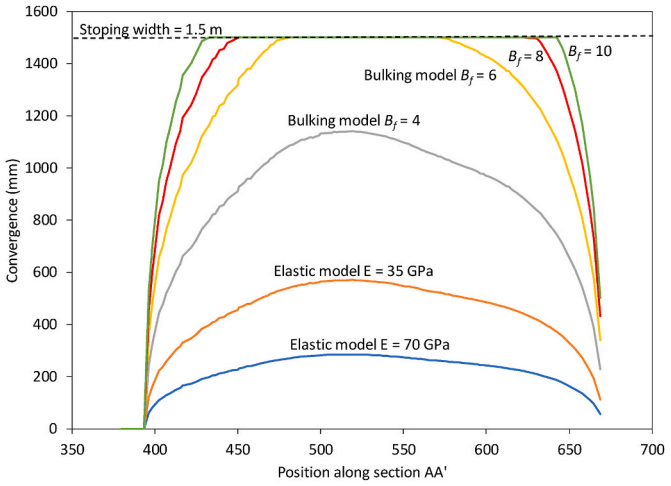

Fig. 11. Convergence profiles along Section AA' (see Fig. 9) for the different models and parameters.

defined by the stoping width. The vertical hangingwall displacement at point X in Fig. 9 was also computed for all models and this is shown in Fig. 12. Note that for an elastic model with E = 70 GPa and a bulking model with E = 70 GPa and $B_f = 4$ (no contact between hangingwall and footwall), the downward displacement is identical, although the convergence as measured in the stope for these two models is completely different (see Fig. 11). This illustrates the value of the bulking model to simulate more realistic convergence magnitudes in displacement discontinuity models without having to resort to an unrealistic reduction in Young's modulus. As soon as closure occurs (for $B_f = 6, 8, 10$), a reaction force is generated according to Eq. (6) and this reduces the downward displacement in the hangingwall as shown in Fig. 12.

The effect of the bulking model and closure was investigated. If closure occurs, stress is regenerated in these parts of the stope and this leads to a reduction of stress on the pillars in the layout. This is illustrated in Fig. 13. Note for example for pillar P11, the APS value reduces from 461 MPa for the elastic model to 371 MPa for a bulking model with $B_f = 10$. Further calibration of the model using closure measurements will be required in order to enable a much better estimate of pillar stresses to be obtained in mature mines.

In Fig. 11, for $B_f = 6$, $B_f = 8$ and $B_f = 10$, the elastic convergence and the bulked material height exceeds the stoping width in the centre of the

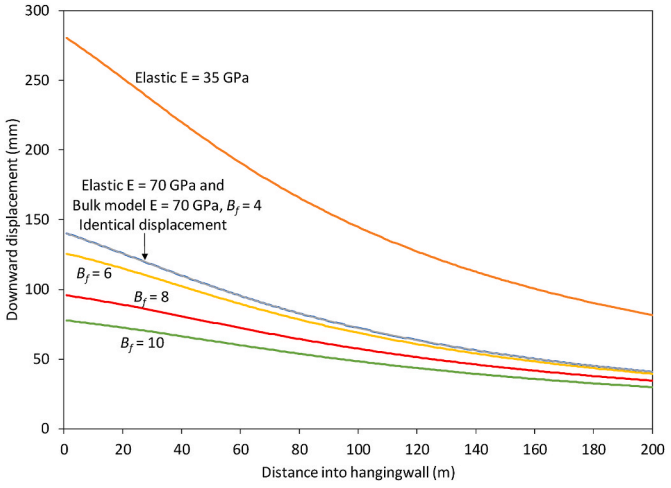

Fig. 12. Vertical downward displacement in the hangingwall at point X in Fig. 9 for the various models and parameters. The distance into the hangingwall is for a line normal to the plane of the reef in Fig. 9.

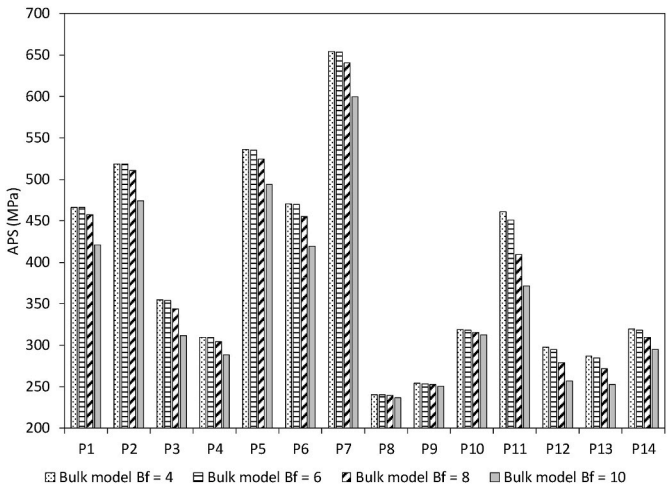

Fig. 13. Reduction in pillar stress for increasing values of the bulking factor. These simulations are for the final pillar geometry in 2020.

stope. The model correctly predicts that this region of closure is larger and closer to the stope face for $B_f = 10$ compared to $B_f = 6$. A reef-normal compressive reaction stress R is generated in these regions according to Eq. (6). This is the value of this constitutive model and the reason for implementing it to simulate this regeneration of stress caused by the closure behaviour shown in Fig. 1 (right). This results in the reduction in stress on the pillars shown in Fig. 13. As mentioned above, however, this model needs careful calibration using underground measurements.

An important test for the proposed model is whether it can replicate the rock mass response and in particular the typical time-dependent closure curves that have been observed in the Bambanani Shaft pillar shown in Fig. 7. The modelling also included a limit equilibrium model to simulate the extensive face crushing shown in Fig. 6. The limit equilibrium model implemented in the TEXAN code has been described in an earlier paper by Napier and Malan[40] and the reader is referred to this reference for additional information.

The area of interest (panel S1) is indicated in Fig. 14 and this area was simulated in detail to test the bulking model. Note that this is only the upper left-hand portion of the larger shaft pillar shown in Fig. 9 (area marked "B"). The face positions in 2022 was used and it is therefore slightly different compared to the outline shown in Fig. 9. Small element sizes were required for the limit equilibrium model and therefore it was not feasible to simulate the entire shaft pillar geometry. The mining outlines were again simplified and the geometry shown in Fig. 14 was simulated. The total number of elements used to simulate this model was 135 132. Triangular elements were used and the average element size was ≈ 0.13 m^2 (see Fig. 15). The remaining modelling parameters are given in Table 3. These parameter values were selected to illustrate the behaviour of the model in relation to the enhanced back area closure and the consequent reduction of stress levels in pillar and excavation face abutments. Future work will be directed to calibrate the model with available field stress measurements. It should be noted that the face of panel S1 is approximately 150 m from the shaft pillar boundary. As there is extensive mining adjacent to the boundary on the other side (left of the boundary), this may affect convergence measurements in panels if they mining close to this boundary. Panel S1 is still far away, however, and this effect is ignored.

The simulated convergence at point A (the position where the closure logger was installed) for two different values of B_f^m is shown in Fig. 16. These simulations are encouraging as the closure profile evolution is very similar to the actual measured convergence results shown in Fig. 7. The convergence in other positions in the panel was also studied. This is illustrated in Fig. 17. Note that position A has the lowest convergence as it is in close proximity to the solid abutment. The convergence at position B indicates large instantaneous convergence jumps during the mining face advance increments. This increment in convergence decreases into the back area as can be seen from the profiles simulated for positions C and D. The largest cumulative magnitude of convergence is at position D and this is correct as the maximum convergence will always be in the centre of the tabular excavation. It is encouraging that these results are in qualitative agreement with the results presented by

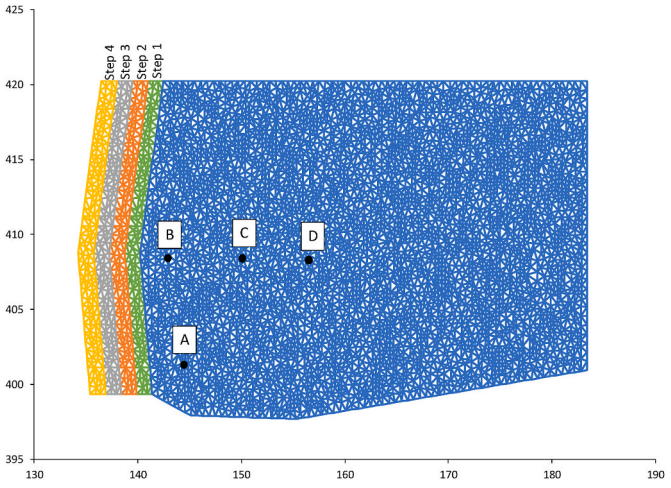

Fig. 15. The triangular mesh used to simulate panel S1 (see Fig. 14). The steps on the left indicate the face advance increments. The simulated time-dependent convergence shown below was recorded at positions A, B, C and D.

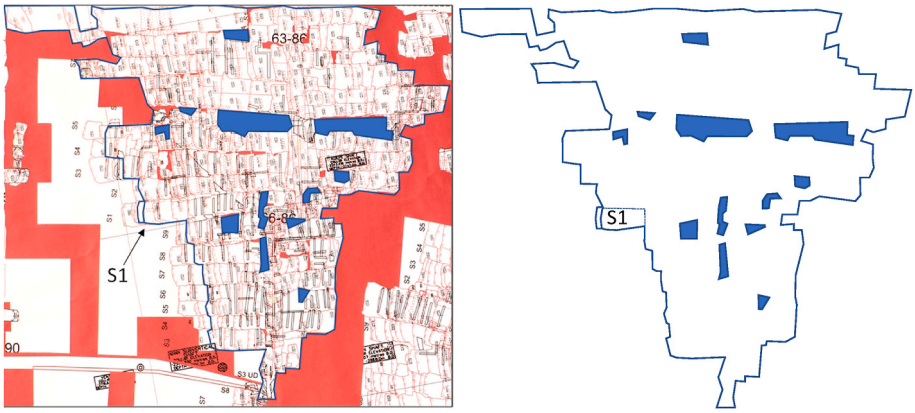

Fig. 14. The upper left section of the Bambanani Shaft pillar. The convergence shown in Fig. 7 was recorded in panel S1.

Table 3
Parameters used for the simulations that included both the limit equilibrium and bulking models. The symbols used for the limit equilibrium model parameters are given in the reference Napier and Malan[40].

Limit Equilibrium Model	Value
Intact strength intercept, σ_c^i	150 MPa
Intact strength slope, m_i	4
Initial residual strength intercept, σ_c^0	100 MPa
Initial residual strength slope, m_0	4
Final residual strength intercept, σ_c^f	10 MPa
Final residual strength slope, m_f	4
Effective seam height, H	1.5 m
Intact seam stiffness modulus, k_s	46667 MPa/m
Fracture zone interface friction angle, φ_i	30°
Half-life, λ	1 h
Bulking Model	
Initial bulking factor, B_f^0	3
Final bulking factor, B_f^m	4 and 5
Compaction modulus, E_0	10 000 MPa
Half-life, λ_B	79.7 h

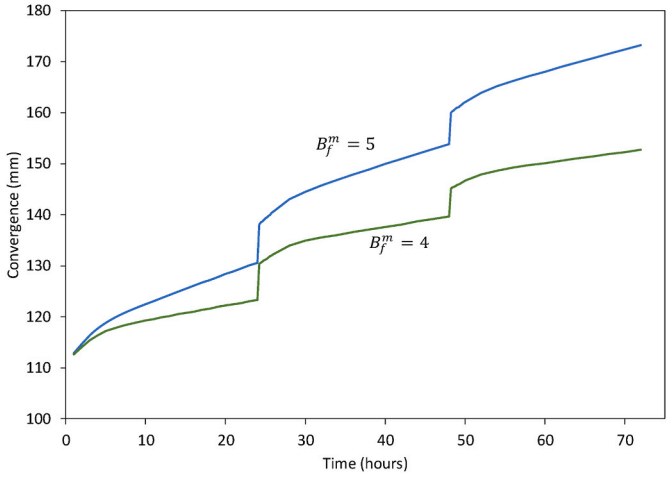

Fig. 16. Simulated time-dependent convergence at position A in Fig. 15.

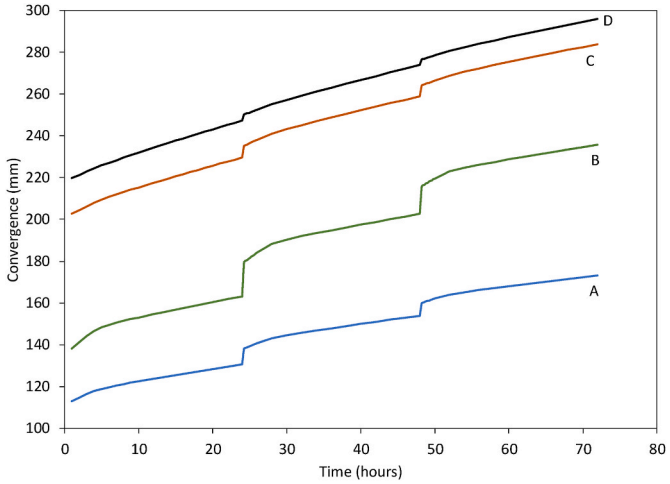

Fig. 17. The effect of position in the panel on simulated convergence. The positions A, B ,C and D are indicated in Fig. 15.

Malan[32] where actual convergence results were obtained at different positions relative to the active mining face in a tabular stope. Malan[32] also reported a decrease in the instantaneous closure component during blasting time if the distance to the face increases. It should be noted, however, that direct comparisons with the actual measured closure data will require additional work as the exact face advance per blast is not known for the area shown in Fig. 15. The size of the incremental face advance significantly affects the closure profile[32]. Further work will require more careful measurement of the underground geometry on a daily basis and the building of more complex models of the panel geometry. This highlights the difficulty of conducting accurate simulations of these tabular stope as a large area needs to be simulated, but fine detail of the geometry, with small incremental face advances, is required on the level of an individual panel.

Fig. 17 highlights an important aspect that needs to be considered when conducting underground convergence monitoring to calibrate the models. The spatial position of the instrumentation needs to be very accurately recorded as the recorded profiles depend greatly on their position in the panel. Ideally, the distance to face also needs to be recorded on an ongoing basis as this will increase, unless the instrument is moved closer to the face.

6. Discussion

Several assumptions were made when developing and testing the constitutive bulking model described in this paper and these are discussed below to guide further research in this area. The objective of this paper was not precise calibration of the model, but a qualitative assessment of the proposed constitutive model to simulate the effects of inelastic rock behaviour around deep tabular stopes.

As described above, it is encouraging that the simulated convergence results are in qualitative agreement with actual convergence results. The time-dependent convergence, as well as the decrease in the instantaneous convergence component during blasting time when the distance to the face increases, can be simulated. Additional work is required for direct comparisons of the modelling results with the actual measured convergence data as the exact face advance per blast is not known for the area studied in this paper. This will involve careful measurement of the underground geometry on a daily basis and the building of more complex models of the precise panel geometry. The work in this paper highlighted the difficulty of conducting accurate simulations of tabular stopes. A large area needs to be simulated, but precise detail of the geometry, with small incremental face advances, is required on the level of individual panels. This requires small elements and is computationally arduous. Alternatively, the background stress induced by mining an extensive area can be estimated for a local "window" region of interest. The fine scale effects in this region can then be simulated using an appropriate computational mesh resolution. This multi-scale aspect was not used in the present paper which has concentrated on the development and qualitative assessment of the proposed back area bulking and stress regeneration model.

An important assumption was that the dip of the reef was simulated to be 0°. The effect of the reef dip in the primitive stress components at the reef horizon is not significant for reef dips lower than 20° and assuming a primitive stress field with vertical and horizontal principal stress directions. For example, if the ratio of the horizontal primitive stress to the vertical primitive stress is 0.5, the primitive stress component normal to the reef plane is approximately five percent lower than the vertical primitive stress when the reef dip is 20°. If the reef dip is 30°, the reef normal primitive stress is 12.5% lower than the vertical primitive stress and the magnitude of the primitive shear stress with respect to the reef plane is about 21.7% of the vertical primitive stress. In this case, the shear stress will induce dip-oriented ride movements that are approximately equal to 21.7% of the reef plane normal closure component. No field evidence is available currently to determine whether the ride movements have a significant effect on the reef-normal bulking behaviour. The use of the empirically calibrated bulking factor, however, subsumes this effect and, as suggested, provides a means of estimating the first order effects of the mined back area stope closure on

stress relief in abutments and pillars. The effect of significant reef plane primitive shear stress is a current topic of research in relation to possible asymmetric pillar edge failure mechanisms.

Other important assumptions used in this study are:

- For the limit equilibrium model, the fracturing is confined to the plane of the reef only.
- An envelope of fractured rock typically surrounds these deep tabular excavations. The current bulking model does not consider the extent of this fracture zone in the hangingwall and footwall. It approximates the effect of bulking, with the various assumptions describe above, only on the plane of the reef.
- The parameter values for the limit equilibrium and bulking models given in the paper are arbitrary values used to test the models. The next step would be more careful calibration using further underground measurements.
- An exponential decay function is used to simulate the time-dependent bulking behaviour. This seems to work well and the time-dependent convergence profiles can be simulated. The use of this exponential decay function requires further verification, however.

The work in this paper highlighted the difficulty of calibrating time-dependent constitutive models using underground closure measurements. The closure data is strongly dependent on the position of the closure meter in the stope. The actual face advance increments and the shape of the geometry is often not recorded owing to the difficult working conditions. This problem needs to be solved as the more complex constitutive models will only be of value if accurate calibrations can be done.

7. Summary

This study explored the use of a novel bulking model, in conjunction with a limit equilibrium model, to simulate observed stope convergence in deep tabular stopes. Encouraging results were obtained that show very good qualitative agreement between the models and convergence data recorded in the Bambanani Gold Mine. The regeneration of stress in back areas of the mine can be more effectively simulated using the proposed bulking model without resorting to an ad hoc modulus reduction strategy. This will enable improved simulations of stresses on remnants and pillars to be conducted.

The practical use of the model will require ongoing calibration of the constitutive models and a programme of routine convergence measurements will have to be implemented at the mines. It is hypothesised that future mine design methodologies will require a greater emphasis on real-time in-panel deformation monitoring. The current work highlighted the importance of accurately recording the spatial position of the instrumentation as the recorded profiles depend sensitively on their position within the mining panel.

Future work will involve the extension of the bulking model to include the effect of backfill placed in the stopes.

Declaration of competing interest

The authors declare that they have no known competing financial interests or personal relationships that could have appeared to influence the work reported in this paper.

Data availability

The authors declare that all the data supporting the findings of this study are available within the article.

Acknowledgements

This work forms part of a PhD study by Yolande Jooste at the University of Pretoria. This work was undertaken under the auspices of the Harmony Gold Chair of Rock Engineering, and the authors would like to thank Harmony Gold for permission to publish this paper.

References

1 Tucker RF, Viljoen RP, Viljoen MJ. A review of the Witwatersrand Basin - the world's greatest goldfield. *Episodes*. 2016;39:104–133.
2 Malan DF, Napier JAL. Rockburst support in shallow-dipping tabular stopes at great depth. *Int J Rock Mech Min Sci*. 2018;112:302–312.
3 Jooste Y, Malan DF. The need for improved layout design criteria for deep tabular stopes. *J S Afr Inst Min Metall*. 2020;120(1):23–32.
4 Malan DF, Napier JAL. A review of the role of underground measurements in the historic development of rock engineering in South Africa. *J S Afr Inst Min Metall*. 2021;121(5):201–216.
5 Denkhaus HG, Hill FG, Roux AJA. A review of recent research into rockbursts and strata movement in deep-level mining in South Africa. *Papers of the Association of Mine Managers of South Africa*. 1958:245–269, 1958–1959.
6 Terzaghi K, Richart FE. Stresses in rock about cavities. *Geotechnique*. 1952;3:57–90, 1952.
7 Ryder JA, Officer NC. An elastic analysis of strata movement observed in the vicinity of inclined excavations. *J S Afr Inst Min Metall*. 1964;64(6):219–244.
8 Ortlepp WD, Cook NGW. The measurement and analysis of the deformation around deep, hard-rock excavations. In: *Proceedings of the International Conference on Strata Mechanics, Columbia University*. New York: Columbia University; 1964.
9 Ortlepp WD, Nicoll A. The elastic analysis of observed strata movement by means of an electrical analogue. *J S Afr Inst Min Metall*. 1964;64:214–235.
10 Cook NGW, Hoek E, Pretorius JPG, Ortlepp WD, Salamon MDG. Rock mechanics applied to the study of rockbursts. *J S Afr Inst Min Metall*. 1966;66:435–528.
11 Hackett P. An elastic analysis of rock movements caused by mining. *Trans Inst Mar Eng*. 1959;118:421–435.
12 Berry DS. An elastic treatment of ground movement due to mining I. Isotropic ground. *J Mech Phys Solid*. 1960;8:280–292.
13 Berry DS. The ground considered as a transversely isotropic material. *Int J Rock Mech Min Sci*. 1964;1:159–167.
14 Berry DS, Sales TW. An elastic treatment of ground movement due to mining II. Transversely isotropic ground. *J Mech Phys Solid*. 1961;9:52–62.
15 Berry DS, Sales TW. An elastic treatment of ground movement due to mining III. Three-dimensional problem, transversely isotropic ground. *J Mech Phys Solid*. 1964;9:8352–8362, 1964.
16 Salamon MDG. Elastic analysis of displacements and stresses induced by the mining of seam or reef deposits – Part I: fundamental principles and basic solutions as derived from idealised models. *J S Afr Inst Min Metall*. 1963;63:128–149.
17 Salamon MDG. Elastic analysis of displacements and stresses induced by the mining of seam or reef deposits – Part II: practical methods of determining displacement, strain and stress components from a given mining geometry. *J S Afr Inst Min Metall*. 1964;64:197–218.
18 Salamon MDG. Elastic analysis of displacements and stresses induced by the mining of seam or reef deposits – Part III: an application of the elastic theory: protection of surface installations by underground pillars. *J S Afr Inst Min Metall*. 1964;64:468–500.
19 Salamon MDG. Elastic analysis of displacements and stresses induced by the mining of seam or reef deposits – Part IV: inclined reef. *J S Afr Inst Min Metall*. 1965;65:319–338.
20 Starfield AM, Fairhurst C. How high-speed computers advance design of practical mine pillar systems. *Eng Min J*. 1968;169:78–84.
21 Plewman RP, Deist FH, Ortlepp WD. The development and application of a digital computer method for the solution of strata control problems. *J S Afr Inst Min Metall*. 1969;70:33–44.
22 Deist FH, Georgiadis E, Moris JPE. Computer applications in rock mechanics. *J S Afr Inst Min Metall*. 1972;72:265–272.
23 Ryder JA, Jager AJ. *A Textbook on Rock Mechanics for Tabular Hard Rock Mines*. Johannesburg: SIMRAC; 2002.
24 Cook NGW. The basic mechanics of rockbursts. *J S Afr Inst Min Metall*. 1963;64:71–81, 1963.
25 Jager AJ, Ryder JA. *A Handbook for Rock Engineering Practice for Tabular Hard Rock Mines*. Johannesburg: SIMRAC; 1999.
26 *International Society for Rock Mechanics: Commission on Terminology, Symbols and Graphic Representation*. ISRM; 1975.
27 Altson BT. Remarks on sand-filling. *Papers of the Association of Mine Managers of South Africa 1931–1936*. 1933:429–432.
28 Mickel RE. *Pressure Bursts. Papers of the Association of Mine Managers of South Africa 1931–1936*. 1935:394–428, 1935.
29 Leeman ER. Some measurements of closure and ride in a stope of the East Rand proprietary mines. *Papers of the Association of Mine Managers of South Africa*. 1958:385–404, 1958–1959.
30 Roux AJA, Denkhaus HG. An investigation into the problem of rockbursts. An operational research project: Part II: an analysis of the problem of rockbursts in deep-level mining. *J Chem Metall Min Soc S Afr*. 1954;55:103–124.

31 Hodgson K. Report on the behaviour of the failed zone ahead of a face, as indicated by continuous seismic and convergence measurements. In: *Research Report No. 31/67. Transvaal and Orange Free State Chamber of Mines Research Organisation*. April 1967.
32 Malan DF. Time-dependent behaviour of deep level tabular excavations in hard rock. *Rock Mech Rock Eng*. 1999;32(2):123–155.
33 Malan DF, Napier JAL, Janse van Rensburg AL. Stope deformation measurements as a diagnostic measure of rock behaviour: a decade of research. *J S Afr Inst Min Metall*. 2007;107:743–765.
34 Walsh JB, Leyde EE, White AJA, Carragher BL. Stope closure studies at West Driefontein gold mine. *International Journal of Rock Mechanics and Mining Sciences and Geomechanical Abstracts*. 1977;14:277–281, 1977.
35 Gurtunca RE, Adams DJ. Determination of the in situ modulus of the rockmass by the use of backfill measurements. *J S Afr Inst Min Metall*. 1991;91(3):81–88.
36 Stacey TR. Written contribution on the paper by Gurtunca, R.E. and Adams, D.J. Determination of the in situ modulus of the rockmass by the use of backfill measurements. *J S Afr Inst Min Metall*. 1991;91(8):286–288.
37 Salamon MDG. Mechanism of caving in longwall coal mining. In: Hustrulid, Johnson, eds. *Rock Mechanics Contributions and Challenges*. Rotterdam: Balkema; 1990.
38 Salamon MDG. Two-dimensional treatment of problems arising from mining tabular deposits in isotropic or transversely isotropic ground. *Int J Rock Mech Min Sci*. 1968;5:159–185.
39 Napier JAL, Malan DF. The computational analysis of shallow depth tabular mining problems. *J S Afr Inst Min Metall*. 2007;107:725–742.
40 Napier JAL, Malan DF. Simulation of tabular mine face advance rates using a simplified fracture zone model. *Int J Rock Mech Min Sci*. 2018;109:105–114.
41 Malan DF, Napier JAL. Reassessing continuous stope closure data using a limit equilibrium displacement discontinuity model. *J S Afr Inst Min Metall*. 2018;118(3):227–234.